Journal of Catalysis 381 (2020) 308–315

Contents lists available at ScienceDirect

Journal of Catalysis

journal homepage: www.elsevier.com/locate/jcat

Green and selective toluene oxidation–Knoevenagel-condensation domino reaction over Ce- and Bi-based CeBi mixed oxide mixtures

Gábor Varga [a,b,*], Ákos Kukovecz [c], Zoltán Kónya [c,d], Pál Sipos [b,e], István Pálinkó [a,b,*]

[a] Department of Organic Chemistry, University of Szeged, Dóm tér 8, Szeged H-6720, Hungary
[b] Materials and Solution Structure Research Group and Interdisciplinary Excellence Centre, Institute of Chemistry, University of Szeged, Aradi Vértanúk tere 1, Szeged H-6720, Hungary
[c] Department of Applied and Environmental Chemistry, University of Szeged, Rerrich Béla tér 1, Szeged H-6720, Hungary
[d] MTA-SZTE Reaction Kinetics and Surface Chemistry Research Group, Rerrich Béla tér 1, Szeged H-6720, Hungary
[e] Department of Inorganic and Analytical Chemistry, University of Szeged, Dóm tér 7, Szeged, H-6720, Hungary

ARTICLE INFO

Article history:
Received 14 August 2019
Revised 3 November 2019
Accepted 8 November 2019

Keywords:
CeBi-oxide solid solutions
Comprehensive structural characterization
Knoevenagel condensation on the solid bases
Toluene oxidation on the Ce-centres
Oxidation and Knoevenagel condensation domino reaction over the mixed CeBi oxides
Environmentally benign conditions

ABSTRACT

Both Bi- and Ce-based CeBi mixed oxides were prepared by a modified sol-gel process from their precursor salts. The mixed as well as the parent oxides were characterized by X-ray diffractometry, Raman, XPS, UV–DRS and X-ray photoelectron spectroscopies, ICP–OES method, scanning and transmission electron microscopies as well as BET surface area, CO_2- and NH_3-temperature-programmed desorption measurements. After characterizing the morphology, the acid-base properties, the oxidation states of the cationic components and the porosity of these structures, their catalytic activities were probed in the Koevenagel condensation of benzaldehyde and diethyl malonate and the toluene oxidation to benzaldehyde reactions. Based on the catalytic activities of the oxides in the individual reactions, a catalyst mixture from the Bi- and Ce-based mixed oxides was used successfully in the toluene to benzaldehyde oxidation and benzaldehyde to benzylidene malonate Knoevenagel condensation domino reaction under environmentally benign conditions.

1. Introduction

Knoevenagel condensation [1] is a still frequently applied reaction in, for instance, the synthesis of some new drugs. They are atorvastatin [2] a well-known cardiovascular pharmaceutical, pioglitazone [3] used to treat diabetes mellitus type 2 or MDL 103371 [4], which is a glycine receptor antagonist for the treatment of stroke to mention just a few. Considering the strict environmental laws and that the pharmaceuticals mentioned are produced on a large scale, greening each reaction step, and thus the Knoevenagel reaction too, was and still is a must.

The environmentally benign improvements of the condensation reaction can be divided into two groups.

The application of environmentally benign solvents like ionic liquids and using alternative methods like solvent-free synthesis, high pressure [5,6], special gaseous catalysts [7] or microwave irradiation [8,9] belong to the first group. Although these methods worked in the laboratory scale, scaling them up to be useful at the industrial level was not possible because of various reasons like the high price of the catalysts. As for now, despite their demonstrated outstanding efficiency, the high price of ionic liquids [10–12] are also against their wide spread use.

The second group is developing water-based reactions. Due to the inexpensive and environmentally friendly nature, water-based reactions [13–15] are desirable even if occasionally, the rate of the reaction is lower than in organic medium. However, if new types of catalysts are devised, which work in aqueous environment, the reaction rate may become comparable to the one running in organic solvent.

In connection with the second group, porous as well as layered structures were probed as catalysts in Knoevenagel reaction. Zeolites [16,17], montmorillonite [18], layered double hydroxides [19,20] and their modified versions [21,22] displayed advantageous features from increasing the selectivity to decreasing the reaction time. However, either the reusability or the general applicability of the catalysts often caused serious problems. Basic mixed oxides such as MgAl [23], NiMo [24] and others [25] have well-known structures, they are easy to synthesize, have outstanding activities and selectivities; nevertheless, stability issues may arise due to excessive leaching. Among them, the CeZr mixed oxide

* Corresponding authors at: Department of Organic Chemistry, University of Szeged, Dóm tér 8, Szeged H-6720, Hungary.
E-mail addresses: gabor.varga5@chem.u-szeged.hu (G. Varga), palinko@chem.u-szeged.hu (I. Pálinkó).

https://doi.org/10.1016/j.jcat.2019.11.011
0021-9517/

[26] was particularly interesting, since short reaction time was needed, and nearly full conversion was reached.

Based on these preliminaries, we planned to synthesize a CeBi mixed oxide to use as catalyst in Knoevenagel reaction and to develop a green synthesis route. The motivation for application of bismuth as dopant was that new studies proved the catalytic potential of Bi-containing systems of basic character [27,28], which should be advantageous in this reaction too. Moreover, in order to establish an economically friendly process, toluene [29] was used as the starting reactant. This way, an eco- and environmentally friendly domino reaction system was created.

2. Experimental

2.1. Materials and syntheses of the oxides

All the chemicals ($Bi(NO_3) \times 5\ H_2O$, $Ce(SO_4)_2 \times 4\ H_2O$, CeO_2, Bi_2O_3, NaOH ethylene glycol) were of reagent grade, and were purchased from Merck or Sigma-Aldrich, and were used without further purification.

The catalysts were prepared by a colloidal phase co-precipitation method. Aqueous -propanol suspensions (V = 25 mL) with varying amounts of $Bi(NO_3) \times 5\ H_2O$ ($n = 6 \times 10^{-5} - 6 \times 10^{-4}$ mol) were made and treated by a 15-minute-long ultrasonic irradiation followed by the addition of 10 mL ethylene glycol to establish a set of sols. After that, the sols were stirred at 50 °C for 60 min. A second suspension of $Ce(SO_4)_2 \times 4\ H_2O$ ($n = 6 \times 10^{-4}$ mol) was also prepared. This suspension was treated the same way as the bismuth-containing systems. Under continuous stirring, the cerium-containing suspension was added dropwise to the bismuth-containing sols. The mixtures were stirred at room temperature for 60 min. Then 0.15 M NaOH (V = 25 mL) was added dropwise until gelation. The gels were stirred at 70 °C for 168 h. The materials obtained were separated by evaporation followed by filtration, washed with hot (~60 °C) distilled water and propanol several times, and dried at 130 °C for 24 h.

2.2. Characterization techniques

X-ray diffraction (XRD) patterns were recorded on a Rigaku XRD-MiniFlex II instrument applying Cu Kα radiation (λ = 0.15418 nm) with 40 kV accelerating voltage at 30 mA.

The morphologies of the freshly prepared samples were studied by scanning electron microscopy (SEM). The SEM images were registered on an S-4700 scanning electron microscope (SEM, Hitachi, Japan) with accelerating voltage of 10–18 kV. More detailed images on the freshly prepared samples, were captured by transmission electron microscopy (TEM). For these measurements, a FEI Tecnai™ G2 20 X-Twin type instrument was used operating at an acceleration voltage of 200 kV.

The Raman spectra were recorded with a Thermo Scientific TM DXRTM Raman microscope at an excitation wavelength of 635 nm applying 10 mW laser power and averaging 20 spectra with an exposition time of 6 s. UV–vis spectra were registered on an Ocean Optics USB4000 spectrometer with a DH-2000-BAL UV–vis–NIR light source measuring diffuse reflectance, and using $BaSO_4$ as reference. The spectra were analysed with the SpectraSuite package.

X-ray photoelectron spectra (XPS) were recorded using a SPECS instrument equipped with a PHOIBOS 150 MCD 9 hemi-spherical electron energy analyser using Al Kα radiation (hν = 1486.6 eV). The X-ray gun was operated at 210 W (14 kV, 15 mA). The analyser was operated in the FAT mode, with the pass energy set to 20 eV. The step size was 25 meV, and the collection time in one channel was 250 ms. Typically, 5–10 scans were added to acquire a single spectrum. Energy referencing was not applied. In all cases the powder-like samples were evenly laid out on one side of a double-sided adhesive tape, the other side being attached to the sample holder of the XPS instrument. The samples were evacuated at room temperature, and then inserted into the analysis chamber of the XPS instrument.

BET surface area measurements were performed on a NOVA3000 (Quantachrome) instrument. The samples were degassed with N_2 at 100 °C for 5 h under vacuum to clean the surface of adsorbed materials. The measurements were performed at the temperature of liquid N_2.

The basic and acid sites of the samples were characterized by temperature-programmed desorption (TPD) measurements using 99.9% CO_2/He and 0.3% NH_3/He, respectively. TPD analysis was performed on a Hewlett-Packard 5890 GC system equipped with thermo-conducting detector. Before the measurements, the mixed oxides were purified by heat treatment at 500 K under He flow.

The actual ratios of metal ions in the mixed oxides were determined by Perkin Elmer Optima 7000DV Inductively Coupled Plasma Optical Emission (ICP–OES) spectrometer. Yttrium internal standard was used for each measurement. Before measurements, few milligrams of the samples measured by analytical accuracy were dissolved in 5 mL cc. HNO_3. After dissolution, the samples were diluted with distilled water to 100 mL and filtered.

Quantitative data for the oxygen content could not be measured, but on the basis of ref. [30], an approximate oxygen content for the phase-pure materials is given.

2.3. General procedures for the catalytic reactions

Knoevenagel condensation: The compound with active methylene group (1.5 mmol), benzaldehyde or its derivative (1.0 mmol) and dodecane as internal standard were dissolved in 3 mL of solvent to get a clear solution. The reaction was quenched after 5 min with 6 N ice-cold HCl. The product was extracted with ethyl acetate (3 × 10 mL). The combined organic extracts were dried using anhydrous sodium sulphate, evaporated under reduced pressure, and assayed on a GC. Conversions in all cases were monitored with respect to the decay of the aldehyde on GC. Hewlett-Packard 5890 chromatograph equipped with a flame ionization detector was employed for the analysis.

Toluene oxidation was carried out as follows: catalyst in 2.3 mL solvent, toluene (8.3 M, 2.7 mL), TBHP (70%, 167 mM) (or other oxidizing agent) were added into the flask. The reaction was carried out at various reaction temperatures and monitored by gas chromatography.

Domino reaction: the reactions were run at the optimized reaction conditions for toluene oxidation. The transformations were followed by gas chromatography.

3. Results and discussion

3.1. Comprehensive structural characterization of the oxides

In order to assign the actual molar ratio for the cationic components of the mixed oxides, elemental analysis was performed by the ICP–OES method (first and second columns of Table 1).

The XRD patterns of the as-prepared CeBi hybrid oxides are shown in Fig. 1. As the patterns obtained attest, the structures of the different CeBi hybrid materials were strongly influenced by the concentrations of the cationic components. The diffraction lines in diffractograms A–C could be indexed as a face-centred cubic fluorite structure [31–34] of CeO_2 (JCPDS No. 43-1002), and no separate crystalline bismuth ion containing phases could be identified, i.e., it is highly probable that Bi(III) ions were incorporated into the ceria lattice.

Table 1
Characteristic information about the single oxides and the CeBi hybrid oxides prepared: [+]measured by ICP–OES, [++]measured by CO_2-TPD, [+++]calculated from XP spectra.

Ce:Bi nominal ratio	Ce:Bi actual ratio[+]	Amount of desorbed CO_2 (mmol/g)[++]	BET surface area (m^2/g)	Ce/Bi ratio on the surface[+++]
CeO_2	nr	0	43	nr
9:1	12:1	0.09	27	4
8:2	10:1	0.27	40	2.6
7:3	9:1*	0.49	52	0.95
6:4	1.3:1	0.61	40	0.7
1:1	1:1.43*	0.94	36	0.4
Bi_2O_3	nr	0	60	nr

* Chemical formula for the phase pure mixed oxides: 9:1 – $Ce_{0.9}Bi_{0.1}O_{1.8}$, 1:1.43 – $Ce_{0.4}Bi_{0.6}O_{1.7}$.

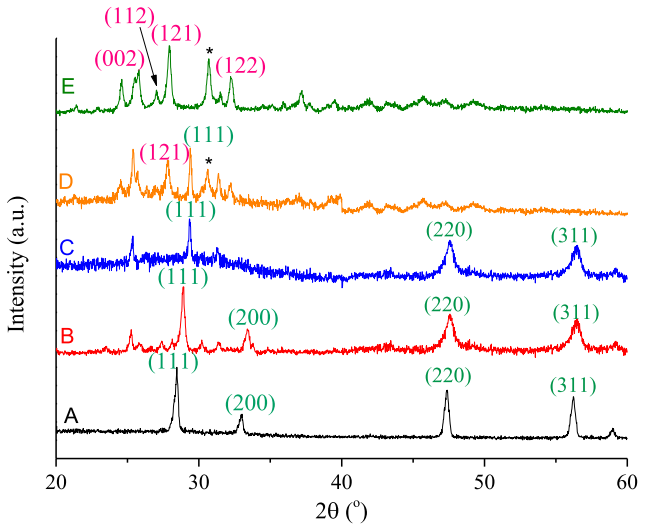

Fig. 1. XRD patterns for CeBi oxide materials with A: 9:1, B: 10:1, C: 12:1, D: 1.3:1, E: 1:1.43 actual Ce:Bi molar ratios.

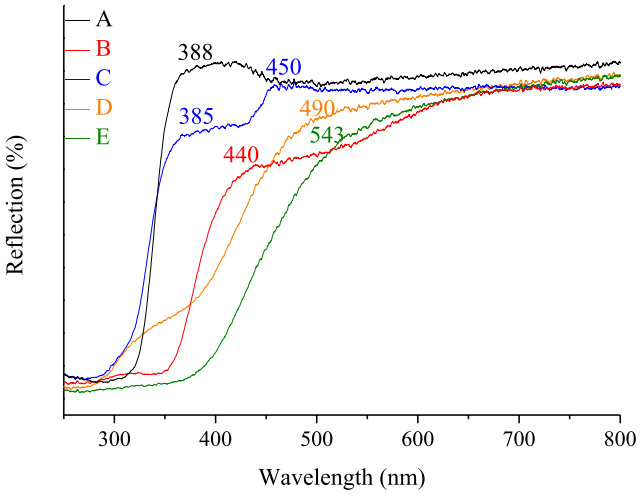

Fig. 2. UV–DR spectra of: A: Bi_2O_3, B: physically mixed Bi_2O_3–CeO_2 of 1:1 ratio, C: CeO_2, D: $Ce_{0.9}Bi_{0.1}O_{1.8}$, E: $Ce_{0.4}Bi_{0.6}O_{1.7}$.

On increasing the Bi(III) concentration, new diffraction lines were observed indicating the appearance of another phase (diffractogram D). Here, the new pattern overlapped with that of fluorite. Diffractogram E corresponding to the material with bismuth ions in excess ($CeBi_{1.43}ox$), displays the five characteristics peaks of the monoclinic α-Bi_2O_3 (JCPDS No. 71-0465). β-Bi_2O_3 phase (JCPD card No. 76-2478) is also detected (marked with *). However, separate ceria phases were not observed. This means that now cerium ions were incorporated into the Bi_2O_3 lattice. The chemical formula of the phase-pure substances are $Ce_{0.9}Bi_{0.1}O_{1.8}$ and $Ce_{0.4}Bi_{0.6}O_{1.7}$. (The oxygen content is an estimate based on ref. [30]). The calculated cell parameters of the phase-pure materials can be found in STable 1 (figures and tables in the Supplementary Material file will be referred as SFigure and STable, respectively).

In Fig. 2, the UV–DRS spectra of the CeO_2, the Bi_2O_3 and the CeO_2–Bi_2O_3 samples are displayed. The reflection edge of CeO_2–Bi_2O_3 in the visible light range were red shifted compared to those of the pure Bi_2O_3 and the pure CeO_2. The light absorption would exhibit increasing red shift with the increase in bismuth content. In order to prove the structural incorporation, a spectrum of physically mixed oxide was also registered. The spectrum can be derived as the sum of the spectra of the physically mixed pure oxides. Both appearing transitions can be attributed to excitonic absorption peaks (388 nm → Bi_2O_3, 440 nm → CeO_2) belonging to the pure starting materials [35,36].

In the Raman spectrum of the pure CeO_2 sample (Fig. 3), in accordance with literature results [37], a single F_{2g} mode vibration could only be observed at 450 cm^{-1}. In the spectrum of $Ce_{0.9}Bi_{0.1}ox$ (spectrum A) this is the predominating band shifted to 440 cm^{-1}. For the fluorite type mixed oxides, it is the decisive band. On the other hand, some intense peaks were also observed at 300 cm^{-1} and 600 cm^{-1} in the fluorite type oxide samples. The presence of vibrations in the region associated with fluorite vibrations for the material with Ce:Bi = 1.3:1 M ratio (spectrum B) suggests the presence of monoclinic structure with oxygen displacement [38]. In the spectrum of the one with Ce:Bi = 9:1 M ratio (spectrum E), the only strong peak in the 100–400 cm^{-1} region was observed at 160 cm^{-1}. This can be ascribed to Bi^{3+} cation motion in [BiO_6] octahedron,

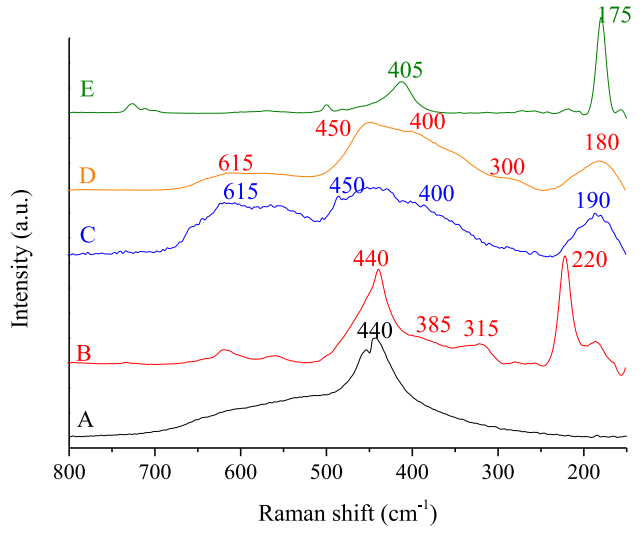

Fig. 3. Raman spectra of for CeBi oxide materials with A: 9:1 ($Ce_{0.9}Bi_{0.1}O_{1.8}$), B: 10:1, C: 12:1, D: 1.3:1, E: 1:1.43 ($Ce_{0.4}Bi_{0.6}O_{1.8}$) actual Ce:Bi molar ratios.

which is described in the literature as the A_{1g} mode [39]. In the higher energy region, a peak at 405 cm^{-1} was observed, and assigned to Bi—O—Bi stretching vibrations in distorted [BiO_6] units [40]. In the spectra of the other mixed oxides with Ce excess (spectra C and D), the characteristic features of the spectra of $Ce_{0.9}Bi_{0.1}O_{1.8}$ and $Ce_{0.4}B_{0.6}O_{1.7}$ are seen, although the corresponding bands were shifted (440 cm^{-1} → 450 cm^{-1}, 405 cm^{-1} → 400 cm^{-1} 175 cm^{-1} → 190 or 180 cm^{-1}) indicating once again that CeBi oxides with mixed phases were produced.

In order to learn about the oxidation states of the guest cations in the phase-pure mixed oxides ($Ce_{0.9}Bi_{0.1}O_{1.8}$, $Ce_{0.4}Bi_{0.6}O_{1.7}$), XPS measurements were performed (Fig. 4). Surprisingly, based on the 3d photoelectron transition of Ce and 4f transition of Bi ions [41–43], it was found that beside Bi(III), Ce(IV)/Ce(III) ions were in the structures. Probably, part of the Ce(IV) ions were oxidized by the ethylene glycol in the synthesis mixture to form Ce(III) [44]. In addition, the incorporation of Ce(III) into the mixed oxide structure inhibited its re-oxidation by air. The results from XPS analysis (last column in Table 1) revealed the presence of much higher percentage of bismuth on and near the surface in all samples than expected indicating that bismuth had a very strong preference to occupy surface sites.

SEM images of the phase-pure mixed oxides are shown in Fig. 5. $Ce_{0.9}O_{0.1}$ox has irregular cauliflower-like shape, while $CeBi_{1.43}$ox has semi regular, rounded cubic shape morphology.

The low BET surfaces indicate that non-porous structures were produced (fourth column in Table 1). The maxima at about 450 K

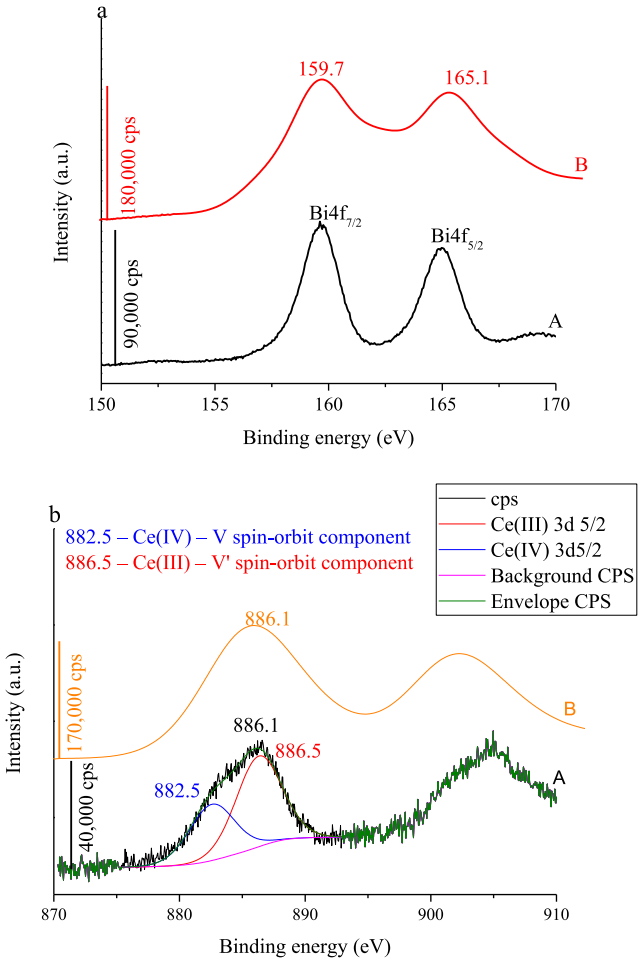

Fig. 4. XP spectra of: A: $Ce_{0.4}Bi_{0.6}O_{1.7}$, B: $Ce_{0.9}Bi_{0.1}O_{1.8}$ mixed oxides; binding energies of (a) Bi species and (b) Ce species.

on the CO_2-TPD profiles (Fig. 6) reveal the presence of moderately basic sites (Table 1) over the surfaces [45], while the pure CeO_2 or the Bi_2O_3 were found to be non-basic. Acid sites were not detected by NH_3-TPD measurements either over the mixed oxide or the single oxide samples. It is seen that the amount of basic sites is significantly lower for the fluorite-type materials than for the monoclinic mixed oxides. These observations and the previously discussed XPS results verify that the basicity of the materials can mainly be attributed to the Bi(III) cations.

3.2. Testing the catalytic behaviour in the Knoevenagel condensation reaction

CeO_2 did not show any activity in the condensation reaction of benzaldehyde and diethyl malonate to produce benzylidene malonate (Scheme 1) or other products under the same reaction conditions as was used for the phase-pure mixed oxides.

The results (Table 2) show strong dependence on the amount of basic sites (determined by CO_2 adsorption and serving as the basis of TOF calculations – see column 3 in Table 1) attributed to the Bi (III) ions in the mixed oxides. It is known that Knoevenagel condensation is a base-catalysed reaction, the basic surface acts as the proton scavenger to generate malonic ester anion, which is the nucleophile attacking at the positively polarised carbonyl carbon (Scheme 2).

Accordingly, the catalytic test reaction was further studied using the $Ce_{0.4}Bi_{0.6}O_{1.7}$ mixed oxide to identify optimum reaction conditions. The conversion of the reaction could be increased up to 80% by increasing the amount of catalyst from 0.005 to 0.02 g (STable 2). The conversion could be further enhanced on applying even larger catalyst loading; however, a drop in selectivity was observed (last row in STable 2). A competing reaction, the Michael addition appeared. Indeed, the benzylidene malonate could play the role of Michael acceptor [46]. Accordingly, in further optimisation 0.02 g catalyst loading was used.

After determining the optimum catalyst loading, various solvents such as ethanol, water, chloroform or acetonitrile were tried. On using chloroform or acetonitrile, negligible conversions were observed. The significantly greener polar protic ethanol was found to be highly efficient. Here, we saw a possibility of further greening the reaction: perhaps, aqueous ethanol or even water may also be good or even better choices. As data in STable 3 shows, aqueous ethanol or water proved to be good solvents; however, ethanol remained the best.

The influence of temperature was investigated in the 25 °C–60 °C temperature range keeping the other parameters fixed (STable 4). The increase of conversion along with the decrease in selectivity was observed on increasing reaction temperature. Due to the higher temperature, from 45 °C, decarboxylation also took place providing with cinnamic acid [47]. Keeping the reaction temperature as low as 25 °C, but increasing the reaction time to 10 h, 92% conversion could be reached maintaining 100% benzylidene malonate selectivity. On further increasing the reaction time at this temperature to 24 h, the conversion could be raised to 98%, still maintaining 100% selectivity. However, 100% conversion and selectivity within reasonable time could be reached at 35 °C reaction temperature.

The recycling properties of the catalyst were studied using the reaction conditions found to be optimal (1.0 eq of benzaldehyde, 1.5 eq of diethyl malonate, 0.02 g of $Ce_{0.4}Bi_{0.6}O_{1.7}$, 35 °C reaction temperature, 360 min reaction time, ethanol as solvent). After a reaction, the catalyst was filtered, washed with ethanol and water several times and dried at 60 °C overnight. The reaction was repeated four times with the above treatments between the runs. Conversions remained 100% or very close to it in the repeated runs, while small gradual losses in selectivities were experienced, but

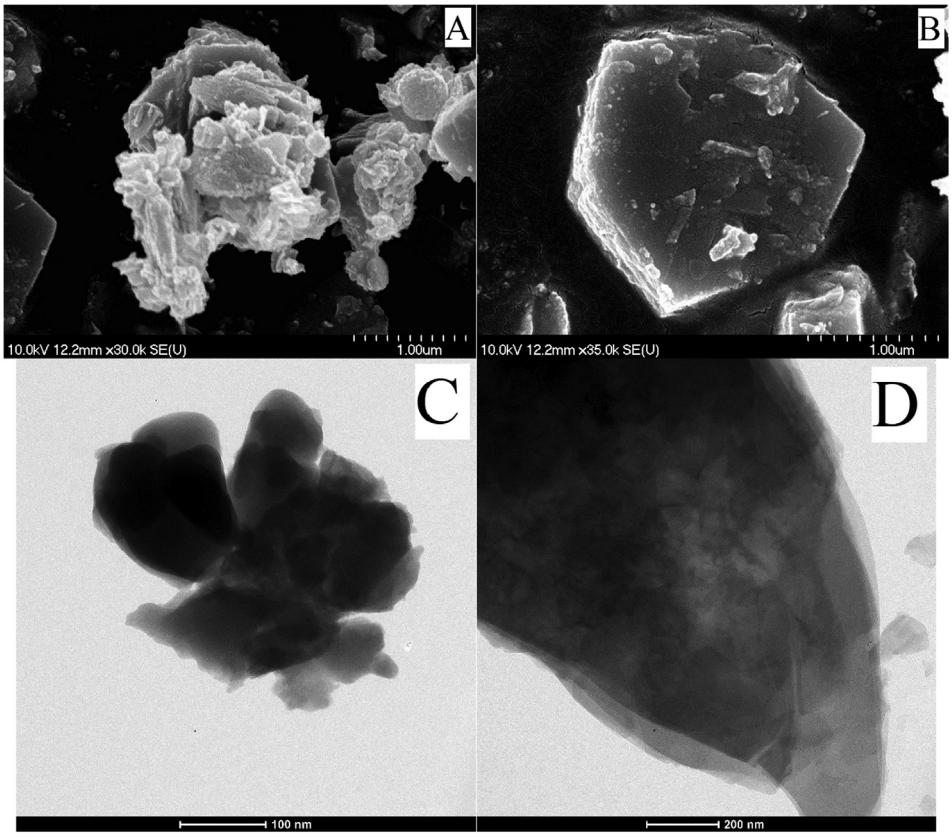

Fig. 5. SEM images: A: $Ce_{0.9}Bi_{0.1}O_{1.8}$, B: $Ce_{0.4}Bi_{0.6}O_{1.7}$; TEM images: C: $Ce_{0.9}Bi_{0.1}O_{1.8}$, D: $Ce_{0.4}Bi_{0.6}O_{1.7}$.

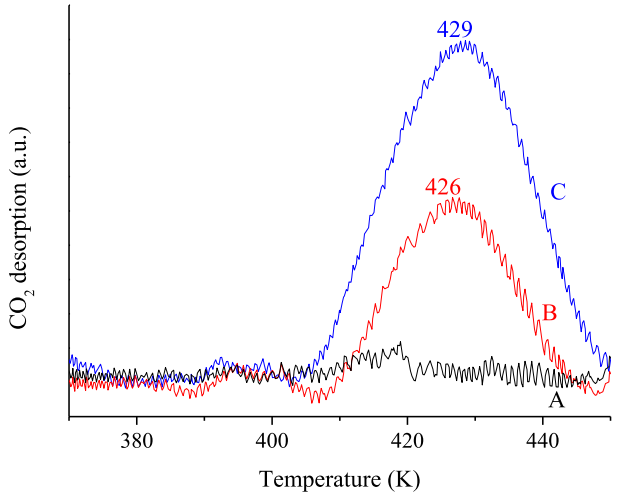

Fig. 6. CO_2-T(emparature)P(rogrammed)D(esorption) spectra: A: CeO_2, B: $Ce_{0.9}Bi_{0.1}O_{1.8}$ and C: $Ce_{0.4}Bi_{0.6}O_{1.7}$.

Table 2
Conversion/TOF and selectivity results of the Knoevenagel condensation between benzaldehyde (1.0 eq) and diethyl malonate (1.5 eq); m_{cat} = 0.015 g, T = 35 °C, t = 180 min in ethanol.

Catalyst	Conversion (%)/TOF (molecules/basic sites/h)	Selectivity (%)
CeO_2	–	–
$Ce_{0.9}Bi_{0.1}O_{1.8}$	17/7.2	100
$Ce_{0.4}Bi_{0.6}O_{1.7}$	**60/13.8**	100
Bi_2O_3	–	–

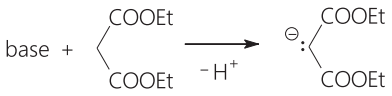

Scheme 2. Deprotonation of diethyl malonate by base or basic sites.

the condensation selectivity was 92% even in the fourth repeated run (Table 3).

The stability of the $Ce_{0.4}Bi_{0.6}O_{1.7}$ catalyst on reuse was monitored by ICP–OES, but measurable leaching of either Ce or Bi ions could not be observed.

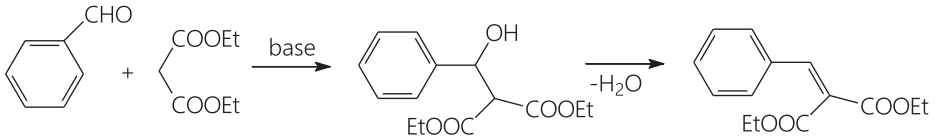

Scheme 1. The Knoevenagel condensation of benzaldehyde and diethyl malonate forming benzylidene malonate as the condensation product.

Table 3
Recycling abilities of the $Ce_{0.4}Bi_{0.6}O_{1.7}$ catalyst – conversion/TOF and selectivity results of the Knoevenagel condensation between benzaldehyde (1.0 eq) and diethyl malonate (1.5 eq); $m_{cat.}$ = 0.02 g, T = 35 °C, t = 360 min, ethanol.

Recycling	Conversion (%)/TOF (molecules/basic sites/h)	Selectivity (%)
1st	100/9.0	100
2nd	99/8.4	94
3rd	100/8.4	93
4th	98/7.8	92

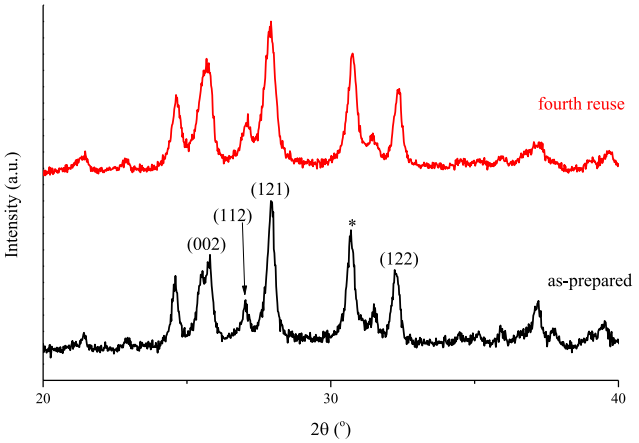

Fig. 7. The X-ray diffractograms of the as-prepared and the recycled $Ce_{0.4}Bi_{0.6}O_{1.7}$ catalyst in the Knoevenagel condensation of benzaldehyde and diethyl malonate.

The original structure of the recycled $Ce_{0.4}Bi_{0.6}O_{1.7}$ mixed oxide was maintained even after the fourth recycling (Fig. 7).

The scope of the condensation reaction was also studied (STable 5). As it is expected, the electron withdrawing groups in the *para* position favour the reaction, since the carbonyl carbon becomes more positive. However, the electron donating groups do the opposite, consequently, the conversions decreased significantly. Michael addition product was observed in these cases. Malononitrile was as good active methylene compound as the malonic ester, while malonic acid was useless in this reaction, since acid-base reaction can take place with the basic catalyst, and malonic acid deprotonated at the carboxylic group is not an active methylene compound any more.

Table 4
Conversion/TOF and selectivity results of toluene oxidation with TBHP (m_{cat} = 0.1 g, T = 110 °C, t = 480 min, solvent-free).

Catalyst	Conversion (%)/TOF (molecules/basic sites/h)	Selectivity (%)
CeO_2	–	–
$Ce_{0.9}Bi_{0.1}O_{1.8}$	11.0/51.0	80
$Ce_{0.4}Bi_{0.6}O_{1.7}$	0.1/0.18	9
Bi_2O_3	–	–

For the above reactions, N_2 atmosphere was needed; without it, benzaldehyde (or its derivatives) was oxidised fast, thus, condensation did not occur [48]. This observation gave the idea to include oxidation in the catalytic test, the oxidation of toluene. If it works producing benzaldehyde, we have one of the reactants for the Knoevenagel condensation. Since diethyl malonate should not get oxidised, it can be added to the reaction mixture together with toluene, and we now have the chance to create a domino reaction system.

3.3. Testing the catalytic behaviour in the oxidation of toluene

For studying the oxidation behaviour of our substances, solvent-free toluene oxidation was tried (Table 4). Initial experiments made it clear that the single oxides (CeO_2 and Bi_2O_3) did not catalyse this reaction even at reflux temperature. The activity $Ce_{0.4}Bi_{0.6}O_{1.7}$ was negligible; however, the ceria-based one was active; however, the $Ce_{0.9}Bi_{0.1}O_{1.8}$ displayed appreciable activity (11% conversion), and remarkable selectivity towards benzaldehyde (80%).

Testing different oxidising agents revealed that *tert*-butyl hydroperoxide (TBHP) could only be applied. Other agents like hydrogen peroxide or O_2 gave no reaction (Table 5, lines 3 and 4). We tried to lower the reaction temperatures to get closer to the temperature of the Knoevenagel reaction (Table 5, line 4), and observed slightly lower activity at 60 °C than at reflux temperature. On lengthening the reaction time at 60 °C, resulted in the remarkable 42% conversion and 90% selectivity in a 24-h reaction (Table 5, line 5). After this run, the catalyst was recycled three times after regenerating it between the runs by filtering, washing with water, then drying at 60 °C. It is shown in the last line of Table 5 that more than 36% conversion of toluene was still maintained even after the third reuse of the catalyst. After the last run, the structure of the catalyst was maintained verified by X-ray diffractometry (Fig. 8).

The scope of the reaction was also studied using toluene derivatives. It was observed that derivatives with electron donating substituent behaved similarly to toluene, while the presence of electron withdrawing substituent prevented the oxidation to occur (STable 6).

For the sake of the possible combination of the oxidation and the condensation reaction, it had to be learnt if the oxidation proceeds in the presence of solvents used for the Knoevenagel reaction or not. It was found that water could be a good solvent achieving similar results to those obtained under solvent-free conditions; however, in ethanol there was no oxidation at all (STable 7).

3.4. Testing the catalytic behaviour in the toluene oxidation–Knoevenagel condensation one-pot, domino reaction

The combination of the two reactions provided over the mixture of the two mixed oxides (0.1 g of $Ce_{0.9}Bi_{0.1}O1_{.8}$ and 0.2 g of $Ce_{0.4}Bi_{0.6}O_{1.7}$) with nice results, when water was the solvent.

Table 5
Effect of the oxidising agent – conversion/TOF and selectivity results of toluene oxidation over $Ce_{0.9}Bi_{0.1}O_{1.8}$ catalyst; m_{cat} = 0.1 g, solvent-free.

Oxidising agent	Temperature (°C)	Reaction time (min)	Recycling	Conversion (%)/TOF (molecules/basic sites/h)	Selectivity (%)
TBHP	110	480	–	11/51.0	80
O_2	110	480	–	–	–
H_2O_2	110	480	–	–	–
TBHP	60	480	–	10/49.2	85
TBHP	60	1440	–	42/73.2	90
TBHP	60	1440	1st	39/67.8	90
TBHP	60	1440	2nd	37/63.0	88
TBHP	60	1440	3rd	36/60.1	87

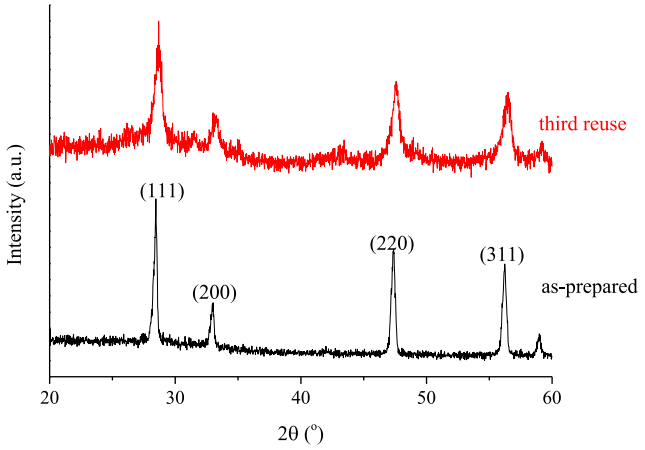

Fig. 8. The X-ray diffractograms of the as-prepared and the recycled $Ce_{0.9}Bi_{0.1}O_{1.8}$ catalyst in the toluene oxidation reaction.

Table 6
Conversion and selectivity results of toluene oxidation to benzaldehyde–Knoevenagel condensation of the in situ formed benzaldehyde and diethyl malonate one pot, domino reaction over $Ce_{0.9}Bi_{0.1}O_{1.8}$–$Ce_{0.4}Bi_{0.6}O_{1.7}$ catalyst system ($m_{cat.}$=(0.1 + 0.2) g, T = 60 °C, t = 1440 min).

Toluene derivative	Solvent	Conversion (%)*	Conversion (%)**	Selectivity (%)
4-Cl-toluene	water	–	–	–
4-NO_2-toluene	water	–	–	–
4-HO-toluene	water	28	84	100
4-CH_3-toluene	water	29	81	100
toluene	water	34	90	100
toluene	toluene	–	–	–

* Conversion for toluene oxidation.
** Conversion for Knoevenagel condensation.

The results obtained are displayed in Table 6. As it is shown, both toluene and its derivatives with electron-donating substituent worked well, provided with the desired condensation products in high yields.

In this system, toluene oxidation took place first over the Bi(III)-based catalyst, then the Knoevenagel condensation with diethyl malonate as the active methylene compound followed. The consecutive reactions proceeded in water, an absolutely green solvent, and was fully selective to the condensation product.

4. Conclusions

The mixture of an exhaustively characterised Ce-based and Bi-based BiCe oxide catalytic system proved to be suitable for promoting a toluene oxidation benzaldehyde–benzaldehyde condensation with diethyl malonate one-pot domino reaction system with 100% selectivity towards the condensation product under mild conditions and in water as the solvent. With this reaction system, many of the requirements of green chemistry were met, such as the use of recyclable heterogeneous catalysts, the application of an environmentally absolutely benign solvent, reaching 100% selectivity and running complex reaction in one pot, without the need for isolating the intermediates.

Declaration of Competing Interest

The authors declared that there is no conflict of interest.

Acknowledgements

This work was supported by the Hungarian Government and the European Union through grant GINOP-2.3.2-15-2016-00013. The financial helps are highly appreciated. One of us, G. Varga thanks for the postdoctoral fellowship under the grant PD 128189.

Appendix A. Supplementary material

Supplementary data to this article can be found online at https://doi.org/10.1016/j.jcat.2019.11.011.

References

[1] E. Knoevenagel, Ueber eine darstellungsweise der glutarsäure, Ber. Dtsch. Chem. Ges. 27 (1894) 2345–2346.
[2] A. Graul, J. Castaner, Atorvastatin calcium, Drugs Future 22 (1997) 956–968.
[3] L.R. Madivada, R.R. Anumala, G. Gilla, S. Alla, K. Charagondla, M. Kagga, A. Bhattacharya, R. Bandichhor, An improved process for pioglitazone and its pharmaceutically acceptable salt, Org. Process Res. Dev. 13 (2009) 1190–1194.
[4] T.J.N. Watson, S.W. Horgan, R.S. Shah, R.A. Farr, R.A. Schnettler, C.R. Nevill, F.J. Weiberth, E.W. Huber, B.M. Baron, M.E. Webster, R.K. Mishra, B.L. Harrison, P.L. Nyce, C.L. Rand, C.T. Goralski, Chemical development of MDL 103371: an N-methyl-d-aspartate-type glycine receptor antagonist for the treatment of stroke, Org. Process Res. Dev. 4 (2000) 477–487.
[5] G. Jenner, Steric effects in high pressure Knoevenagel reactions, Tetrahedron Lett. 42 (2001) 243–245.
[6] N.E. Agafonov, I.P. Sedishev, A.V. Dudin, A.A. Kutin, G.A. Stashina, V.M. Zhulin, Henry condensation under high pressure 2. Effect of aromatic aldehyde type and pressure on the yield of ω-nitrostyrenes and secondary processes, Bull. Acad. Sci. USSR, Div. Chem. Sci. (Engl. Transl.) 40 (1991) 366–372.
[7] G. Kaupp, M.R. Naimi-Jamal, J. Schmeyers, Tetrahedron 59 (2003) 3753–3760.
[8] D. Bogdal, Coumarins: Fast synthesis by knoevenagel condensation under microwave irradiation, J. Chem. Res. (S) (1998) 468–469.
[9] P. Lidström, J. Tierney, B. Wathey, J. Westman, Microwave assisted organic synthesis– a review, Tetrahedron 57 (2001) 9225–9283.
[10] J.R. Harjani, S.J. Nara, M.M. Salunkhe, Lewis acidic ionic liquids for the synthesis of electrophilic alkenes via the Knoevenagel condensation, Tetrahedron Lett. 43 (2002) 1127–1130.
[11] R.V. Hangarge, D.V. Jarikote, M.S. Shingare, Knoevenagel condensation reactions in an ionic liquid, Green Chem. 4 (2002) 266–268.
[12] P. McNeice, A.C. Marr, P.C. Marr, M.J. Earle, K.R. Seddon, Binary alkoxide ionic liquids, ACS Sustain. Chem. Eng. 6 (2018) 13676–13680.
[13] T. Murase, Y. Nishijima, M. Fujita, Cage-catalyzed Knoevenagel condensation under neutral conditions in water, J. Am. Chem. Soc. 134 (2011) 162–164.
[14] X. Dong, Y. Hui, S. Xie, P. Zhang, G. Zhou, Z. Xie, Schiff base supported MCM-41 catalyzed the Knoevenagel condensation in water, RSC Adv. 3 (2013) 3222–3226.
[15] B.C. Ranu, R. Jana, Ionic Liquid as Catalyst and Reaction Medium – A Simple, Efficient and green procedure for Knoevenagel condensation of aliphatic and aromatic carbonyl compounds using a task-specific basic ionic liquid, Eur. J. Org. Chem. 16 (2006) 3767–3770.
[16] X. Zhang, E.S.M. Lai, B. Martin-Aranda, K.L. Yeung, An investigation of Knoevenagel condensation reaction in microreactors using a new zeolite catalyst, Appl. Catal. A 261 (2004) 109–118.
[17] J. Liang, Z. Liang, R. Zou, Y. Zhao, Heterogeneous catalysis in zeolites, mesoporous silica, and metal-organic frameworks, Adv. Mater. 29 (2017) 1701139–1701159.
[18] F. Bigi, L. Chesini, R. Maggi, G. Sartori, Montmorillonite KSF as an inorganic, water stable, and reusable catalyst for the Knoevenagel synthesis of coumarin-3-carboxylic acids, J. Org. Chem. 64 (1999) 1033–1035.
[19] B.M. Choudary, M.L. Kantam, V. Neeraja, K.K. Rao, F. Figueras, L. Delmotte, Layered double hydroxide fluoride: a novel solid base catalyst for C-C bond formation, Green Chem. 3 (2001) 257–260.
[20] Y. Jia, Y. Fang, Y. Zhang, H.N. Miras, Y.F. Song, Classical Keggin intercalated into layered double hydroxides: facile preparation and catalytic efficiency in Knoevenagel condensation reactions, Chem. Eur. J. 21 (2015) 14862–14870.
[21] Y. Horiuchi, T. Toyao, M. Fujiwaki, S. Dohshi, T.H. Kim, M. Matsuoka, Zeolitic imidazolate frameworks as heterogeneous catalysts for a one-pot P-C bond formation reaction via Knoevenagel condensation and phospha-Michael addition, RSC Adv. 5 (2015) 24687–24690.
[22] T. Li, H. Miras, Y.F. Song, Polyoxometalate (POM)-layered double hydroxides (LDH) composite materials: design and catalytic applications, Catalysts 7 (2017) 260–276.
[23] A. Corma, V. Fornes, R.M. Martin-Aranda, F. Rey, Determination of base properties of hydrotalcites: condensation of benzaldehyde with ethyl acetoacetate, J. Catal. 134 (1992) 58–65.
[24] W. Zhou, M. Liu, Q. Zhang, Q. Wei, S. Ding, Y. Zhou, Synthesis of NiMo catalysts supported on gallium-containing mesoporous Y zeolites with different gallium contents and their high activities in the hydrodesulfurization of 4,6-dimethyldibenzo-thiophene, ACS Catal. 7 (2017) 7665–7679.

[25] K.R. Kloetstra, M. Van Laren, H. van Bekkum, Binary caesium–lanthanum oxide supported on MCM- 41: a new stable heterogeneous basic catalyst, J. Chem. Soc., Faraday Trans. 93 (1997) 1211–1220.
[26] G. Postole, B. Chowdhury, B. Karmakar, K. Pinki, J. Banerji, A. Auroux, Knoevenagel condensation reaction over acid–base bifunctional nanocrystalline $Ce_xZr_{1-x}O_2$ solid solutions, J. Catal. 269 (2010) 110–121.
[27] P. Malik, D. Chakraborty, Bi (III)-catalyzed C-S cross-coupling reaction, Appl. Organomet. Chem. 26 (2012) 557–561.
[28] M.F. Nizah, Y.H. Taufiq-Yap, U. Rashid, S.H. Teo, Z.S. Nur, A. Islam, Production of biodiesel from non-edible Jatropha curcas oil via transesterification using Bi_2O_3–La_2O_3 catalyst, Energy Conv. Manag. 88 (2014) 1257–1262.
[29] J. Liu, S. Zou, H. Wang, L. Xiao, H. Zhao, J. Fan, Synergistic effect between Pt(0) and Bi_2O_{3-x} for efficient room-temperature alcohol oxidation under base-free aqueous conditions, Catal. Sci. Technol. 7 (2017) 1203–1210.
[30] L. Bourja, B. Bakiz, A. Benlhachemi, M. Ezahri, J.C. Valmalette, S. Villain, J.R. Gavarri, J. Optoelectron. Adv Mater. – Symp. 3 (2011) 110–113.
[31] K. Sardar, H.Y. Playford, R.J. Darton, E.R. Barney, A.C. Hannon, D. Tompsett, J. Fisher, R.J. Kashtiban, J. Sloan, S. Ramos, G. Cibin, R.I. Walton, Nanocrystalline cerium-bismuth oxides: synthesis, structural characterization, and redox properties, Chem. Mater. 22 (2010) 6191–6201.
[32] L. Bourja, B. Bakiz, A. Benlhachemi, M. Ezahri, S. Villain, O. Crosnier, C. Favotto, J.-R. Gavarri, Structural, microstructural and surface properties of a specific CeO_2–Bi_2O_3 multiphase system obtained at 600°C, J. Solid State Chem. 184 (2011) 608–614.
[33] M. Prekajski, Z. Dohčvić-Mitrović, M. Radović, B. Babić, J. Pantić, A. Kremenović, B. Matović, Nanocrystaline solid solution CeO_2–Bi_2O_3, J. Eur. Ceram. Soc. 32 (2012) 1983–1987.
[34] F. Cao, Q. Dong, C. Li, J. Chen, X. Ma, Y. Huang, D. Song, C. Ji, Y. Lei, Electrochemical sensor for detecting pain reliever/fever reducer drug acetaminophen based on electrospun $CeBiO_x$ nanofibers modified screen-printed electrode, Sens. Actuators B 256 (2018) 143–150.
[35] R. Hirani, C.A. Hogarth, Excitonic absorption in cerium phosphate glasses, J. Mater. Sci. Lett. 8 (1989) 150–152.
[36] L. Li, B. Yan, CeO_2–Bi_2O_3 nanocomposite: two-step synthesis, microstructure and photocatalytic activity, J. Non-Cryst. Solids 355 (2009) 776–779.
[37] A. Martinez-Arias, M. Fernandez-Garcia, L.N. Salamanca, R.X. Valenzuela, J.C. Conesa, J.J. Soria, Structural and redox properties of ceria in alumina-supported ceria catalyst supports, J. Phys. Chem. B 104 (2000) 4038–4046.
[38] J.R. McBride, K.C. Hass, B.D. Poindexter, W.H.J. Weber, Raman and X-ray studies of $Ce_{1-x}RE_xO_{2-y}$, where RE=La, Pr, Nd, Eu, Gd, and Tb, Appl. Phys. 76 (1994) 2435–2441.
[39] L. Baia, R. Stefan, J. Popp, S. Simon, W. Kiefer, Vibrational spectroscopy of highly iron doped B_2O_3–Bi_2O_3 glass systems, J. Non-Cryst. Solids 324 (2003) 109–117.
[40] M. Subhadra, P. Kistaiah, Infrared and Raman spectroscopic studies of alkali bismuth borate glasses: Evidence of mixed alkali effect, Vib. Spectrosc. 62 (2012) 23–27.
[41] R. Wang, H. Xu, X. Liu, Q. Ge, W. Li, Role of redox couples of Rh(0)/$Rh^{\delta+}$ and Ce^{4+}/Ce^{3+} in CH_4/CO_2 reforming over Rh–CeO_2/Al_2O_3 catalyst, Appl. Catal. A 305 (2006) 204–210.
[42] X. Luo, R. Wang, J. Ni, J. Lin, B. Lin, X. Xu, K. Wei, Effect of La_2O_3 on Ru/CeO_2-La_2O_3 catalyst for ammonia synthesis, Catal. Lett. 133 (2009) 382–387.
[43] Y. Ding, F. Yang, L. Zhu, N. Wang, H. Tang, Bi^{3+} self-doped $NaBiO_3$ nanosheets: facile controlled synthesis and enhanced visible light photocatalytic activity, Appl. Catal. B 164 (2015) 151–158.
[44] N. Al-Haq, A.C. Sullivan, J.R.H. Wilson, Oxidation of alcohols using cerium (IV) alkyl phosphonate modified silica, Tetrahedron Lett. 44 (2003) 769–771.
[45] P. Kustrowski, L. Chmielarz, E. Bozek, M. Sawalha, F. Roessner, Acidity and basicity of hydrotalcite derived mixed Mg–Al oxides studied by test reaction of MBOH conversion and temperature programmed desorption of NH_3 and CO_2, Mater. Res. Bull. 39 (2004) 263–281.
[46] E.D. Bergmann, D. Ginsburg, R. Pappo, Organic Reactions, Vol. X, Wiley, New York, 1959, p. 179.
[47] K.M. Parida, D. Rath, Amine functionalized MCM-41: an active and reusable catalyst for Knoevenagel condensation reaction, J. Mol. Catal. A 310 (2009) 93–100.
[48] W.M.H. Sachtler, The mechanism of the catalytic oxidation of some organic molecules, Catal. Rev. 4 (1971) 27–52.